Application of electric and electromagnetic methods to the definition of the Campi Flegrei caldera (Italy)

Rosa Di Maio ([1]), **Domenico Patella** ([1]), **Zaccaria Petrillo** ([2]), **Agata Siniscalchi** ([3]), **Gianpaolo Cecere** ([1]) **and Prospero De Martino** ([2])

([1]) *Dipartimento di Scienze Fisiche, Università «Federico II», Napoli, Italy*

([2]) *Osservatorio Vesuviano, Ercolano, Napoli, Italy*

([3]) *Dipartimento di Geologia e Geofisica, Università di Bari, Italy*

Abstract

The results of an analysis of Dipolar Geoelectrical (DG), Magnetotelluric (MT) and Self-Potential (SP) data collected over the emerged portion of the Campi Flegrei (CF) caldera (South Italy) are presented. The DG and MT data are from previous surveys, while the SP data have been recently collected during a survey consisting of 265 pickup land sites. Although the emerged part of the CF caldera appears as a highly inhomogeneous structure, a few simple features have been highlighted through an integrated analysis of subsets of consistent data. A well resolved feature is the structural pattern of the caldera depression along a roughly E-W profile, deduced from a 2D combined interpretation of the MT and DG soundings. Resistivity dispersion effects have also been observed at both ends of this profile. They have been ascribed to the presence of hydrothermally altered zones related to the main fracture systems bordering the caldera. A pressure/temperature source body at a mean depth of about 5 km bsl under the Bay of Pozzuoli has been inferred from the analysis of the 3D SP tomography imaging.

Key words *applied geophysics – electric and electromagnetic methods – Campi Flegrei caldera*

1. Introduction

The Campi Flegrei (CF) volcanic area is located in South Italy around the western urban territory of Naples. With the islands of Ischia and Procida-Vivara it belongs to the Phlegraean Volcanic District, where the beginning of activity is estimated older than 150 ka (Gillot *et al.*, 1982). It is a resurgent nested caldera that resulted from the two main collapses of decreasing magnitude which followed the eruptions of the Campanian Ignimbrite (37 ka) and the Neapolitan Yellow tuff (12 ka) (Orsi *et al.*, 1996). Historical episodes like the Mount Nuovo eruption in 1538 (Di Vito *et al.*, 1999), the brady-seismic crises of 1970-1972 and 1982-1984 (Orsi *et al.*, 1999a) and the persistent hydrothermal and fumaroles manifestations (Martini *et al.*, 1991) reflect a still intense activity within the CF caldera (CFc).

The CF area has been intensively investigated from the volcanological point of view (Di Girolamo *et al.*, 1984; Rosi and Sbrana, 1987; Orsi *et al.*, 1996; Di Vito *et al.*, 1999). Additional indications have been obtained from seismological (Postpischl, 1985; Aster *et al.*, 1992; De Natale and Pingue, 1992; Orsi *et al.*, 1999a), ground deformation (Berrino *et al.*, 1984; De

Mailing address: Prof. Domenico Patella, Dipartimento di Scienze Fisiche, Università «Federico II», Complesso Universitario Monte S. Angelo, Via Cinthia, 80126 Napoli, Italy; e-mail: patella@na.infn.it

Natale and Pingue, 1992; Orsi *et al.*, 1999a,c), gravity (Cassano and La Torre, 1987; Barberi *et al.*, 1991), magnetic (Cassano and La Torre, 1987; Orsi *et al.*, 1999b), deep temperature (Chelini and Sbrana, 1987; Wohletz *et al.*, 1999) and heat flow (Corrado *et al.*, 1998) data. The results of all these studies strengthen the hypothesis that the CFc is still a highly hazardous volcano. However, the knowledge of the geophysical structure and dynamics of the CF system is not yet complete. High-resolution investigations have long been required within the caldera, mainly beneath the first 3-4 km of depth.

To contribute to fill this gap, this paper presents the main electric properties of the emerged part of the CFc. Indeed, the application of electric and electromagnetic (EM) survey methods in volcanic environments is justified by the strong dependence of resistivity on the physical state of rocks and the high sensitivity of the electrical and EM methods in detecting fracture and fault systems, besides lithological variations.

In the CFc, electric and EM ground surveys are affected by three unavoidable disturbing factors. The first factor is the intense urbanisation that makes the area a rather continuous source of electrical and EM noise. The second factor is a diffuse presence of near-surface geological inhomogeneities that are the sources of high scattering of data in the survey diagrams. The third factor is the impossibility of disposing of a dense station network, due to both intense urbanisation and very rough topography especially close to the caldera boundaries and the numerous volcanic cones.

Notwithstanding these difficulties, the results of our analysis contribute to draw a reference model of the CFc. This model will provide useful constraints for the design and execution of a new marine EM survey that has been recently planned in order to explore the submerged portion of the caldera in the Bay of Pozzuoli.

2. Magnetotelluric interpretation strategy by dipolar geoelectrical soundings

We carried out an analysis of the Dipolar Geoelectrical (DG) survey data reported in Fedi *et al.* (1986). In particular, we analysed two conjugate sounding pairs aligned about N-S (DG1 and DG2) and WNW-ESE (DG3 and DG4) (see fig. 1). The DG sounding curves are drawn in fig. 2a,b. The two main features emerging from the scattered DG diagrams are a close similarity between the N-S conjugate curves DG1 and DG2 that show a logarithmic slope exceeding 45°, and a clear unconformity between the WNW-ESE conjugate curves DG3 and DG4. These two features likely suggest the existence of a 2D shallow resistivity structure with a nearly N-S elongation direction. Such evidence can be used to find a strategy for a preliminary simplified interpretation of the magnetotelluric (MT) soundings as follows.

In the 2D case, the MT impedance tensor after rotation takes the antidiagonal form

$$Z = \begin{pmatrix} 0 & Z_{xy} \\ Z_{yx} & 0 \end{pmatrix} \qquad (2.1)$$

that corresponds to two EM polarisations, known as the TE (Transverse Electric) mode with electric field parallel to strike and TM (Transverse Magnetic) mode with magnetic field parallel to strike. The accumulation of electric charges on the lateral discontinuities will notably deform the TM mode response compared with the 1D MT response that we would obtain if the lateral boundaries were not present. On the contrary, the TE mode response will be less affected and will appear closely similar to the 1D MT response (Wannamaker *et al.*, 1984). This means that a simplification in the analysis of a 2D structure by a 1D MT inversion scheme can only be permitted using the TE mode. We have considered this approach and adopted the 1D Bostick inversion method to obtain preliminary modelled sections across the CF MT profiles.

In 1D Bostick inversion, the relationship between resistivity ρ and depth z beneath a MT sounding station is approximated as

$$\rho(z) \cong \left[\frac{d}{dz} \left(\frac{z}{\rho_a} \right) \right]^{-1} = \rho_a \frac{2+m}{2-m}, \qquad (2.2)$$

where ρ_a is the MT apparent resistivity in the

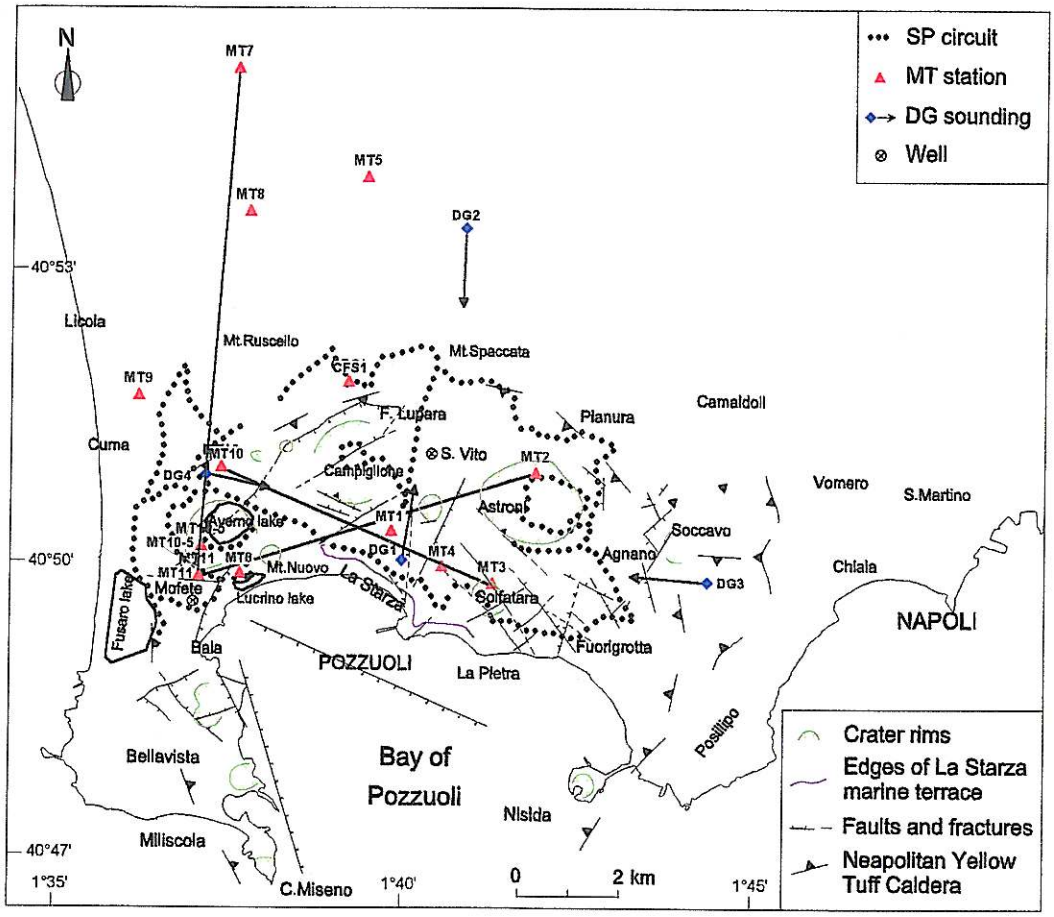

Fig. 1. The Campi Flegrei survey area. The dotted circuits refer to the self-potential survey. The red triangles indicate the magnetotellurics sounding stations. The blue diamonds with arrows indicate the dipole geoelectric sounding stations and expansion axes, respectively.

specified mode and m is computed as

$$m = \frac{d \log \rho_a}{d \log \sqrt{T}} \qquad (2.3)$$

The effect of Bostick algorithm is to smooth away sharp resistivity contrasts and give a continuous resistivity-*versus*-depth profile. Owing to its simplicity and robustness, the 1D Bostick method is currently used to generate fast electric images of the subsoil.

Now, we consider the N-S profile including the soundings MT7, MT8, MT9, MT10, MT10-5 and MT11 (fig. 1). This MT profile is parallel to the coastline bordering the CFc westwards. Figure 3a shows the N-S TE mode apparent resistivity pseudosection, obtained using the MT sounding curves reported by Hunsche *et al.* (1981). Since the shoreline is an evident E-W resistivity crossover, we had one more reason for the MT TE mode curves to be approximated by a 1D Bostick inversion.

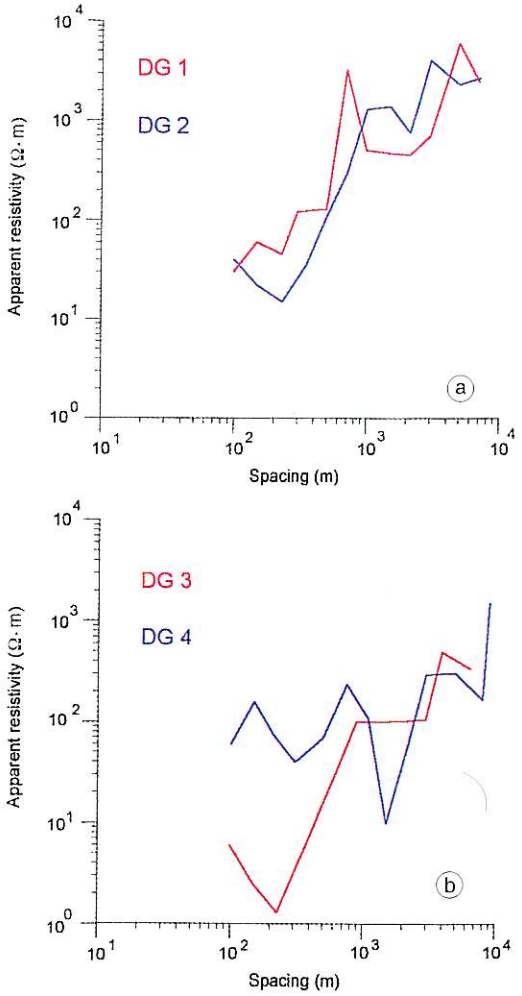

Fig. 2a,b. The dipole geoelectrical sounding diagrams (redrawn after Fedi *et al.*, 1986). Two pairs of conjugate sounding curves are reported: the pair DG1 and DG2 along a nearly N-S direction (a) and the pair DG3 and DG4 along a nearly E-W direction (b).

Figure 3b shows a 2D envelope of the set of 1D Bostick resistivity-depth profiles below the MT stations along the N-S profile. We observe a nearly 1D resistivity distribution in the small range 4-10 Ω·m along the entire profile down to a depth of about 1 km. Thus, regarding the dimensionality point of view, the MT shallow pattern closely conforms to the main feature of the N-S DG diagrams. This N-S lateral uniformity appears, however, abruptly violated in the deeper southern part of the profile, between soundings MT11 and MT10. In fact, at a depth of about 1 km we notice a resistive intrusion steeply dipping northward to about 5 km in depth. We suspect, however, that this marked lateral feature is actually an artefact caused by the use of an inversion approach that neglects resistivity frequency dispersion. Indeed, dispersion phenomena in a conductive layer overlying a resistive substratum cause an abnormal decrease of the MT apparent resistivity before it starts rising toward the resistive asymptote for longer periods. Such a decrease is spread over a period range much larger than the normal range for a conductive non-dispersive layer having the same DC resistivity and thickness as the dispersive layer (Di Maio *et al.*, 1991). Therefore, the resulting effect of a non-dispersive Bostick inversion can be either a fictitious increase in thickness and conductivity of the conductive block, erroneously assumed as non-dispersive, or a fictitious upward migration of the bottom conductive-to-resistive boundary. Patella *et al.* (1991) already suggested considering dispersion effects in the interpretation of MT soundings in the CF area. The authors also emphasised the role of a joint DG-MT analysis to quantify dispersion anomalies in volcano-geothermal areas. This peculiar aspect will be clarified in more detail in the next section.

To conclude this section we briefly present the WNW-ESE line including the stations MT10, MT1, MT4 and MT3, which is nearly orthogonal to the previous profile. Figure 4a shows the WNW-ESE TE mode apparent resistivity pseudosection, contoured using the MT data reported by Hunsche *et al.* (1981) and Monaco *et al.* (1986). A notably more articulated lateral pattern of the electric structure appears now from the surface downwards. The shallow features of the CFc in the nearly E-W direction seem to confirm the inhomogeneous pattern already deduced from the analysis of the DG curves. We do not show the 1D Bostick inversion of this profile, because it was modelled by a more refined 2D dispersive approach, which will be discussed in the next section.

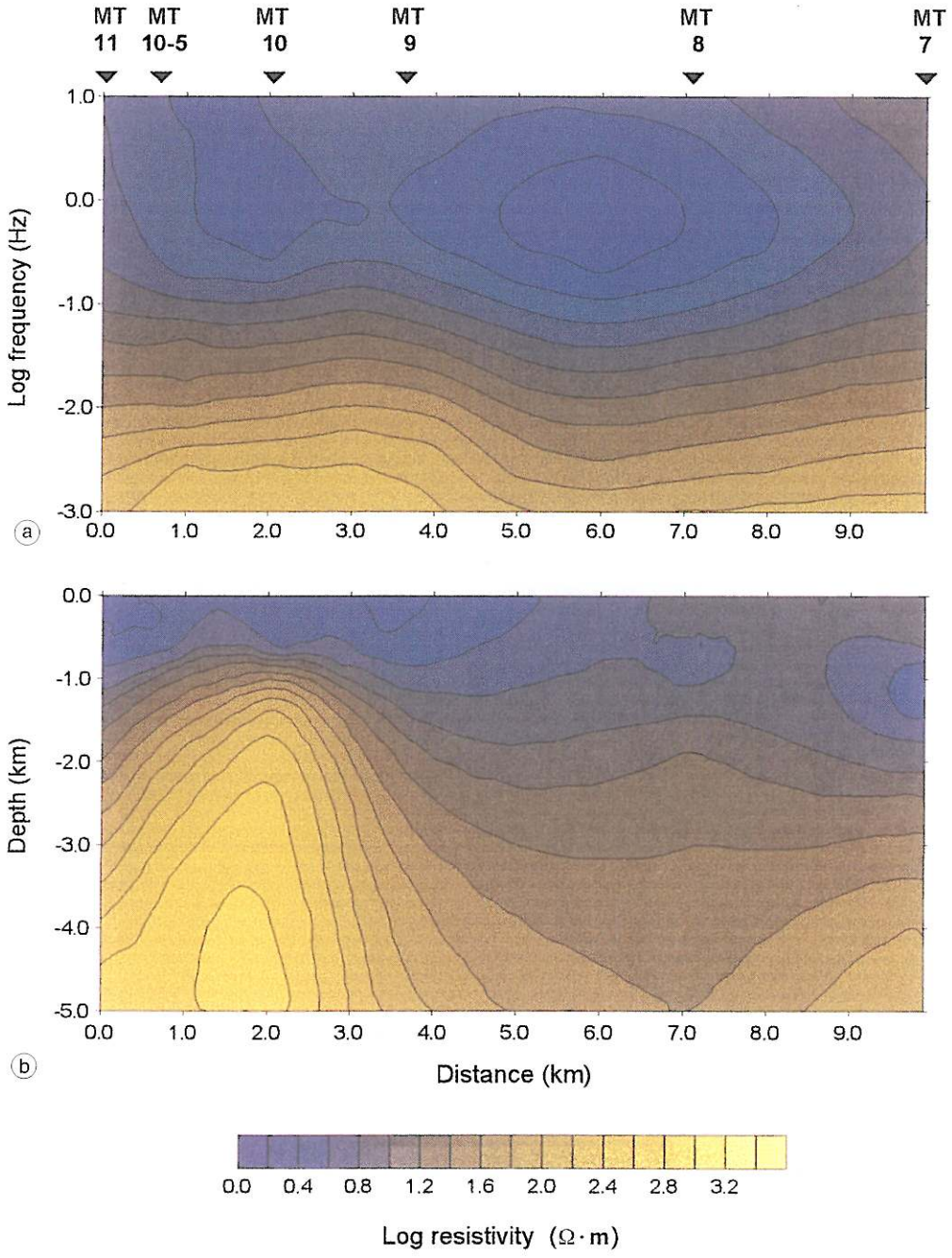

Fig. 3a,b. The magnetotelluric qualitative and quantitative interpretation along a nearly N-S profile including the soundings MT7, MT8, MT9, MT10, MT10-5 and MT11. The sounding data are taken from Hunsche *et al.* (1981). The TE mode apparent resistivity pseudosection (a) and 1D Bostick inversion (b).

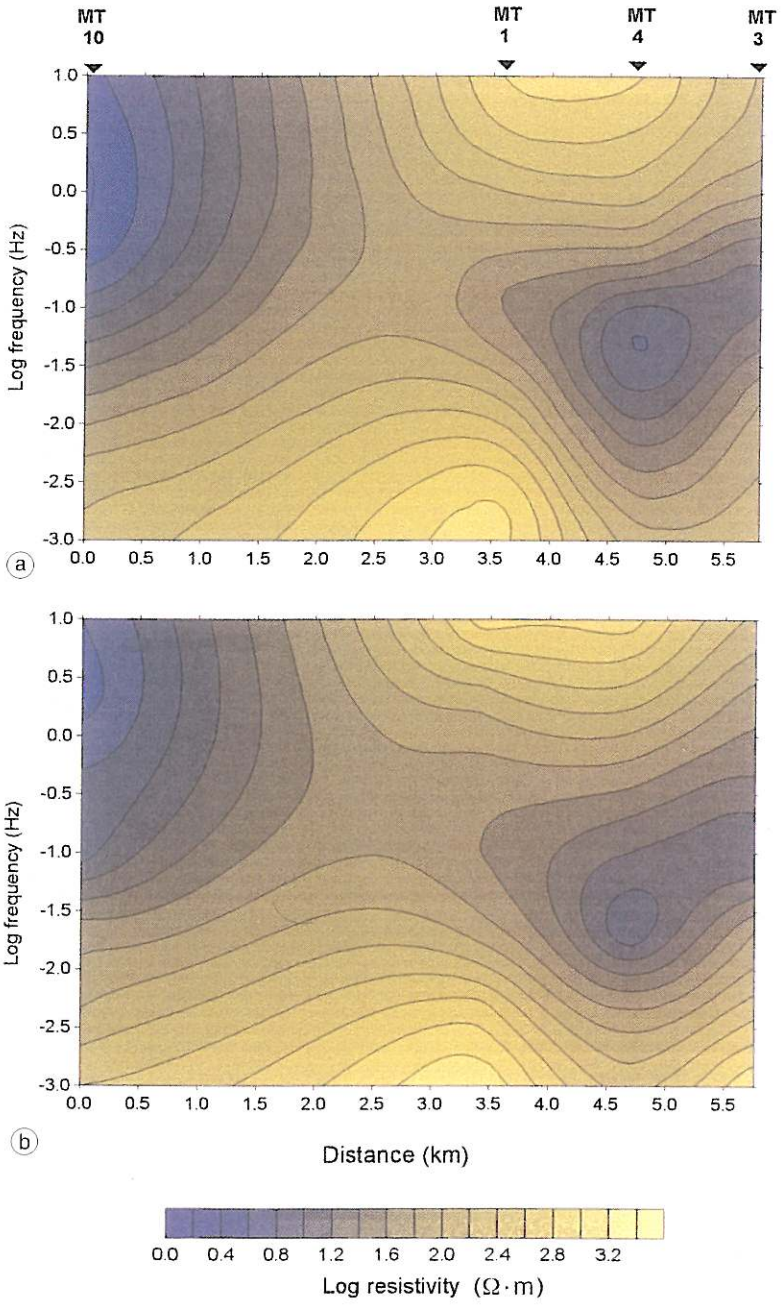

Fig. 4a,b. The magnetotelluric qualitative and quantitative interpretation along a nearly E-W profile including the soundings MT10, MT1, MT4 and MT3. The sounding data are taken from Hunsche *et al.* (1981) and Monaco *et al.* (1986). The TE mode apparent resistivity field pseudosection (a) and synthetic pseudosection reconstructed from the model of fig. 7 (b).

3. DG-MT joint modelling including dispersion

Qualitatively speaking, the MT high frequency band provides penetration depths for the EM waves comparable with those reached by DC currents in deep DG soundings. If resistivity frequency dispersion is present, the MT response will be more or less affected depending on the intensity and depth of the dispersion phenomena, while the DG method will never be affected simply because it operates in a steady regime (Patella, 1987). However, the presence of unknown dispersion effects cannot generally be recognised using MT data alone. Indeed, any MT dispersive response can be equivalent to many other responses of structurally different but non-dispersive situations. This kind of physical equivalence can readily be noted considering for instance the gentle shapes of the 1D MT dispersive apparent resistivity and phase curves depicted in fig. 5a,b (redrawn after Patella *et al.*, 1991). The background MT non-dispersive curve pair, corresponding with the same 1D layered structure, is also depicted in fig. 5a,b. This MT curve pair can in principle always be simulated by a transformation of the apparent resistivity diagram of a DG field sounding performed at the same site (Patella, 1987). Summarizing, two operative statements can be made. The first is that, generally, the presence of resistivity dispersion effects cannot be proved considering only the shape of the apparent resistivity and phase curves of MT soundings. Without knowing the nature and amplitude of the dispersion effects the quantitative analysis of MT soundings can be rather arbitrary. The second statement is that the joint interpretation of DG and MT sounding curves obtained at the same site permits us to solve the ambiguity. Actually, one only needs to transform the DG curve into the equivalent synthetic MT curve set. If original and simulated MT curve sets do not conform to each other and both amplitude and shape of the resulting discrepancy meet the resistivity dispersion theory (Patella, 1993), the original MT curve set can be modelled using dispersion parameters, *e.g.* of Cole-Cole type. An example of this approach applied to the CFc is given in fig. 6a,b (redrawn after Patella *et al.*, 1991), where a 1D dispersive interpretation of the pair of soundings MT10 and DG4 is illustrated. The fitting model was selected from the set of 1D MT dispersive curves drawn in fig. 5a,b.

The DG results previously presented clearly indicate that the N-S direction can locally be assumed as the elongation axis of the main CF resistivity structure. An improved DG-MT joint modelling can thus be made using a 2D algorithm. Here we limit the 2D approach to the WNW-ESE line, which is the only profile including DG stations (DG4, DG1 and DG3). Firstly we stress that no reasonable DG-MT solution could be obtained by a 2D non-dispersive modelling of the section. Hence, we confirm the opportunity to include resistivity frequency dispersion effects in the 2D analysis of the whole line. This hypothesis is also largely supported by mesostructural observations (Orsi *et al.*, 1996, 1999a; Di Vito *et al.*, 1999), which indicate an uplift of blocks confined within fault systems nearly orthogonal to the edges of the WNW-ESE profile. Active faults, fracturing and fluid circulation in volcano-geothermal areas are potential sources of resistivity frequency dispersion phenomena (Mauriello *et al.*, 1996).

For the 2D modelling we used a standard finite difference forward algorithm, modified in such a way as to compute the contributions to the global MT response due to dispersive cells (Mauriello *et al.*, 1996). Figure 7 shows the results of the 2D dispersive model along the WNW-ESE profile through the CFc. The electrical structure at depth below 3÷4 km appears uniform with a resistivity of some thousands $\Omega \cdot m$ and a flexure in the middle part of the profile, beneath soundings MT1, MT4 and MT3. A conductive basin (some tens of $\Omega \cdot m$) that shows a similar flexure and a progressive thinning towards the borders of the profile overlies this basement. These two structures appear as if they had been flexed by the laterally confined, high resistivity (about 4000 $\Omega \cdot m$) body, located in the central part of the profile between 0 and 3 km of depth. This body contrasts eastward a weakly less resistive zone (about 1000 $\Omega \cdot m$) and westward a piled structure with an average lower resistivity. The whole sequence is overlain by a thin low resistivity overburden.

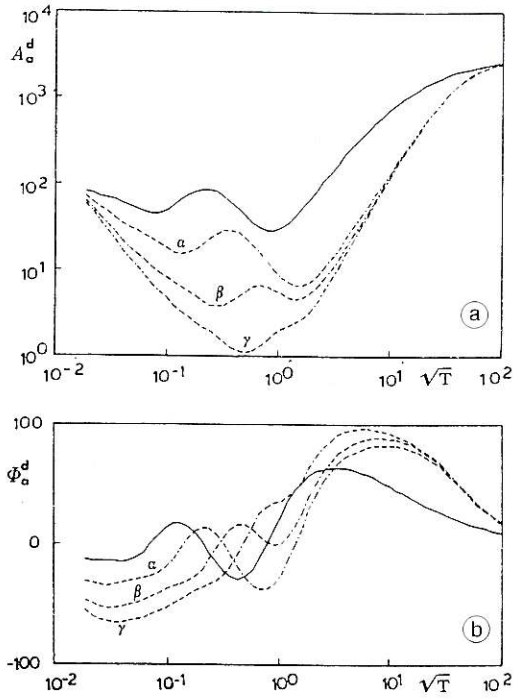

Fig. 5a,b. Theoretical magnetotelluric master curves (amplitudes in $\Omega \cdot$ m in fig. 5a and phases in degrees in fig. 5b) without resistivity frequency dispersion (full lines) and including dispersion effects (curves α, β, γ). A 1D six-layer sequence is considered with the following DC resistivities in $\Omega \cdot$ m from top to bottom: 90, 40, 950, 10, 20 and 3000. The full 2nd layer and the first 230 m of the 4th layer are assumed to be dispersive. The Cole-Cole parameters chargeability m, time constant τ and frequency factor c for the 2nd and 4th layer are respectively: $m = 0.7$ (α), 0.93 (β), 0.98 (γ); $\tau = 500$ s; $c = 0.6$ and $m = 0.9$; $\tau = 10000$ s; $c = 0.6$ (redrawn after Patella *et al.*, 1991).

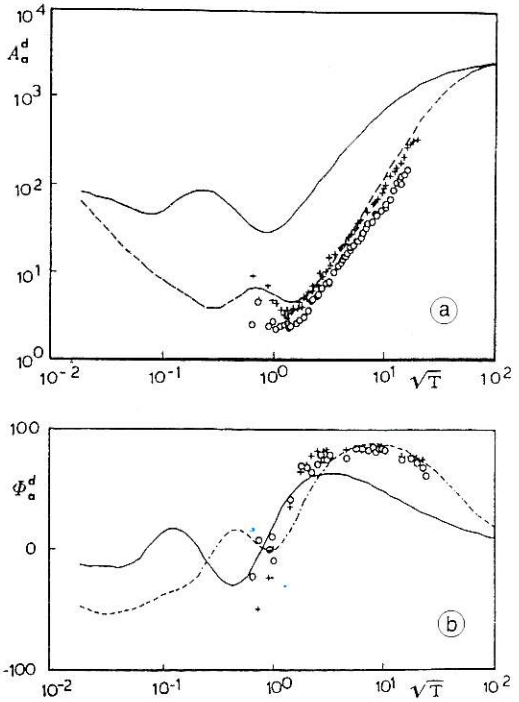

Fig. 6a,b. Magnetotelluric diagrams relative to the sounding MT10 (amplitude in $\Omega \cdot$ m in fig. 6a and phases in degrees in fig. 6b). Crosses and circles refer to the original amplitude and phase field data in the two orthogonal reference directions. The full lines in fig. 6a,b are the synthetic amplitude and phase non-dispersive curves deduced from an expanded interpretation of the geoelectrical sounding DG4 shown in fig. 2a,b. The dashed lines in fig. 6a,b are the apparent amplitude and phase dispersive diagrams fitting to the observed data. They correspond to the curves β in fig. 5a,b (redrawn after Patella *et al.*, 1991).

The prismatic resistive body (about 4 km wide) likely consists of dry volcanic rocks characterized by a low degree of fracturation and/or a network of disconnected pores and fissures. Dispersive zones border it. The dispersion effects are likely due to a forced current circulation through fissures totally occluded by metallic-type mineral particles (Chelini and Sbrana, 1987). A widespread system of disseminated electrolyte-mineral interfaces is a well-known source of redox reactions when an electric current is forced to flow through a self-sealed system. These reactions are not as rapid as the ionic current flow in the electrolytic solution (Parasnis, 1997). The result is a continuous piling up of ionic charges at each interface, known as electrode polarisation that actually acts as an added resistance along the current path. This added resistance increases as the frequency of the current flow decreases, thus giving rise to

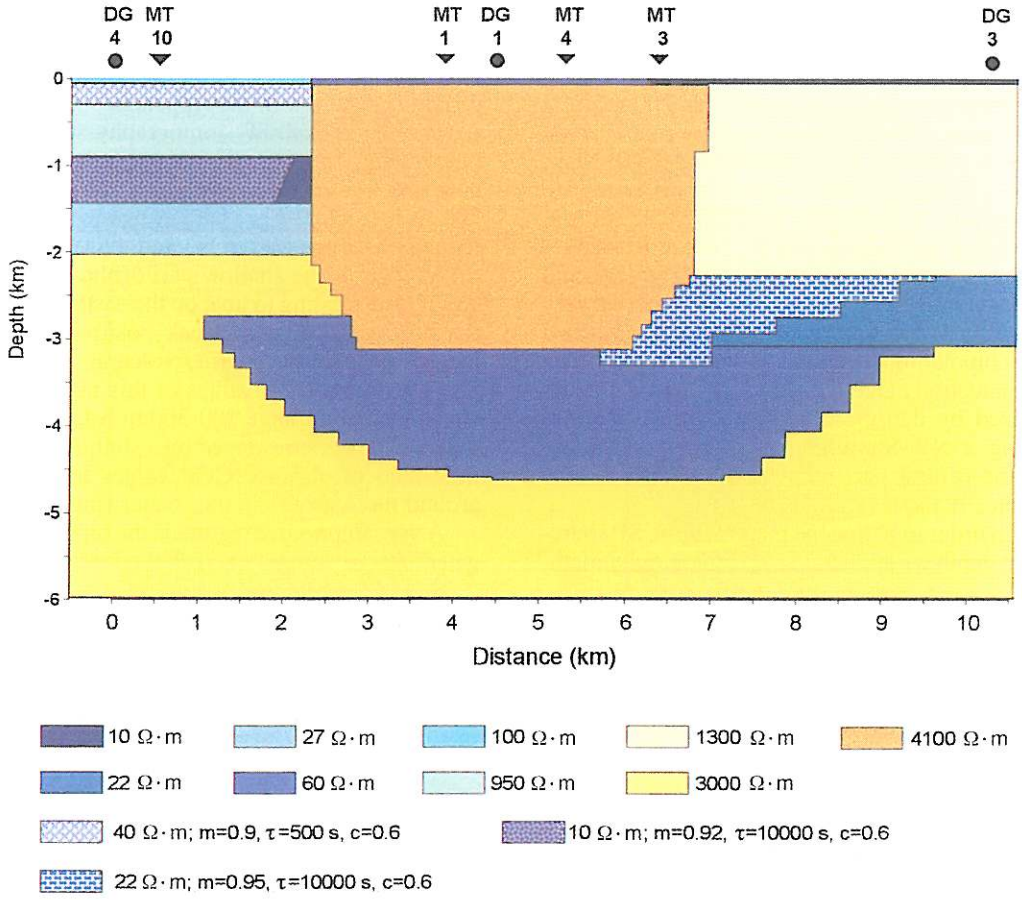

Fig. 7. Joint 2D interpretation with resistivity frequency dispersion of a nearly E-W profile including the magnetotelluric soundings MT10, MT1, MT4 and MT3 and the dipolar geoelectrical soundings DG4, DG1 and DG3.

resistivity frequency dispersion in MT soundings (Mauriello *et al.*, 1996).

Finally, worth commenting is that the discovered dispersive zones confine eastwards with the Solfatara volcano and westwards with the Mofete zone. The Solfatara crater is very well known for its widespread and impressive fumaroles and thermal springs. The Mofete zone is one the most interesting geothermal area within the CFc, since the temperatures measured in wells exceed 300 °C at about 1500 m in depth (Chelini and Sbrana, 1987).

The high reliability of the 2D dispersive model of fig. 7 can be readily appreciated by comparing the synthetic TE mode pseudosection corresponding with the interpreted 2D model (fig. 4b) with the field TE pseudosection previously discussed (fig. 4a).

4. 3D self-potential tomography

The Self-Potential (SP) field survey was carried out along a branched circuit consisting of

265 measurement sites (dots in fig. 1) irregularly distributed over an area of 11×7 km^2 within the emerged portion of the CFc. The spread between two consecutive points was 200 m.

Figure 8 shows the SP survey map, which was drawn using a standard approach (Di Maio *et al.*, 1996). The most remarkable features are the short wavelength anomalies about the Averno Lake, Monte Nuovo, Monte Rusciello, Montagna Spaccata, Gauro-Campiglione and Astroni. All these anomalies are located very close to volcanic vents. They are superimposed on a bipolar long wavelength regional field. The demarcation band of this bipolar field is characterized by dense crowding of the SP isolines along a NW-SE direction, closely coinciding in the central part with the La Starza marine terrace (Cinque *et al.*, 1984).

In order to define the pattern of the SP sources at depth we applied the 3D tomography method suggested by Patella (1997a,b), which is based on the concept of charge occurrence probability (COP). A brief outline of this tomographic procedure is reported in the Appendix.

The 3D probability tomography was computed using two different depth scales. Figure 9a shows a set of images between 100 m asl and 800 m bsl, while fig. 9b investigates the deep features between 600 m bsl and 4200 m bsl.

As regards the shallow part of the CFc (fig. 9a), it is interesting to note on the eastern side of the horizontal slices a weak positive nucleus located beneath the Astroni volcanic structure. The maximum COP values of this nucleus occur in the depth range 200-300 m bsl. The positive nucleus is surrounded by a slightly perceptible halo of negative COP values located all around the Astroni circular crater rim.

A very impressive feature is the bipolar elongated charge anomaly across the La Starza ter-

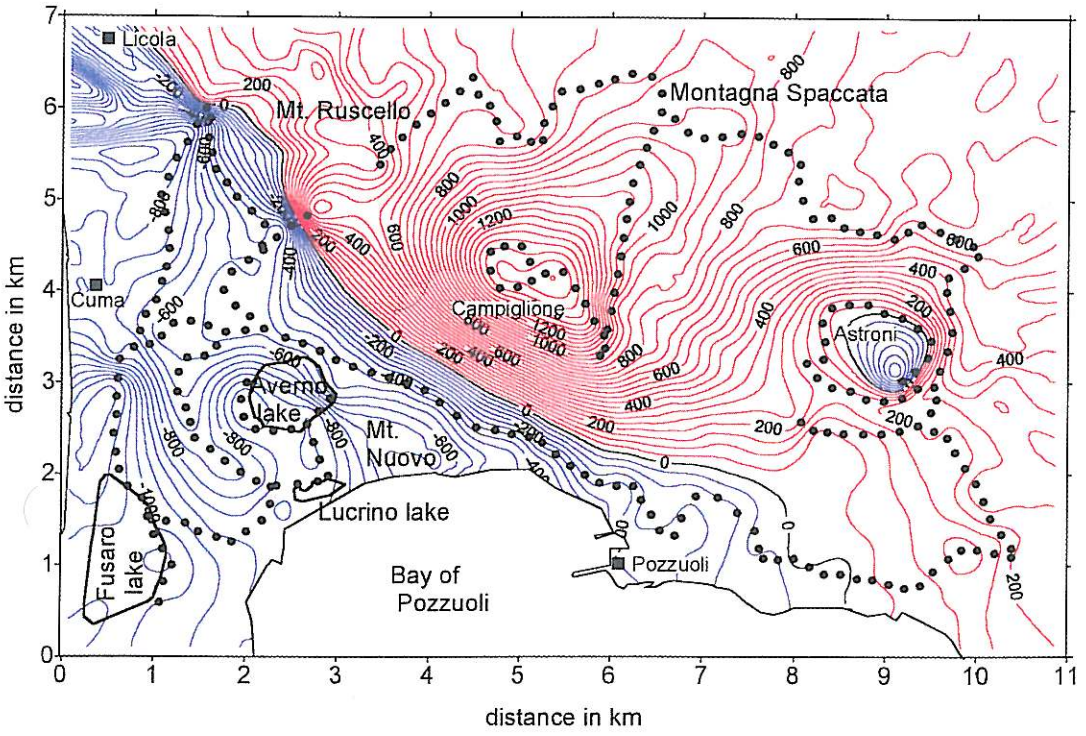

Fig. 8. The self-potential survey map. Red and blue isolines represent positive and negative SP values in mV, respectively.

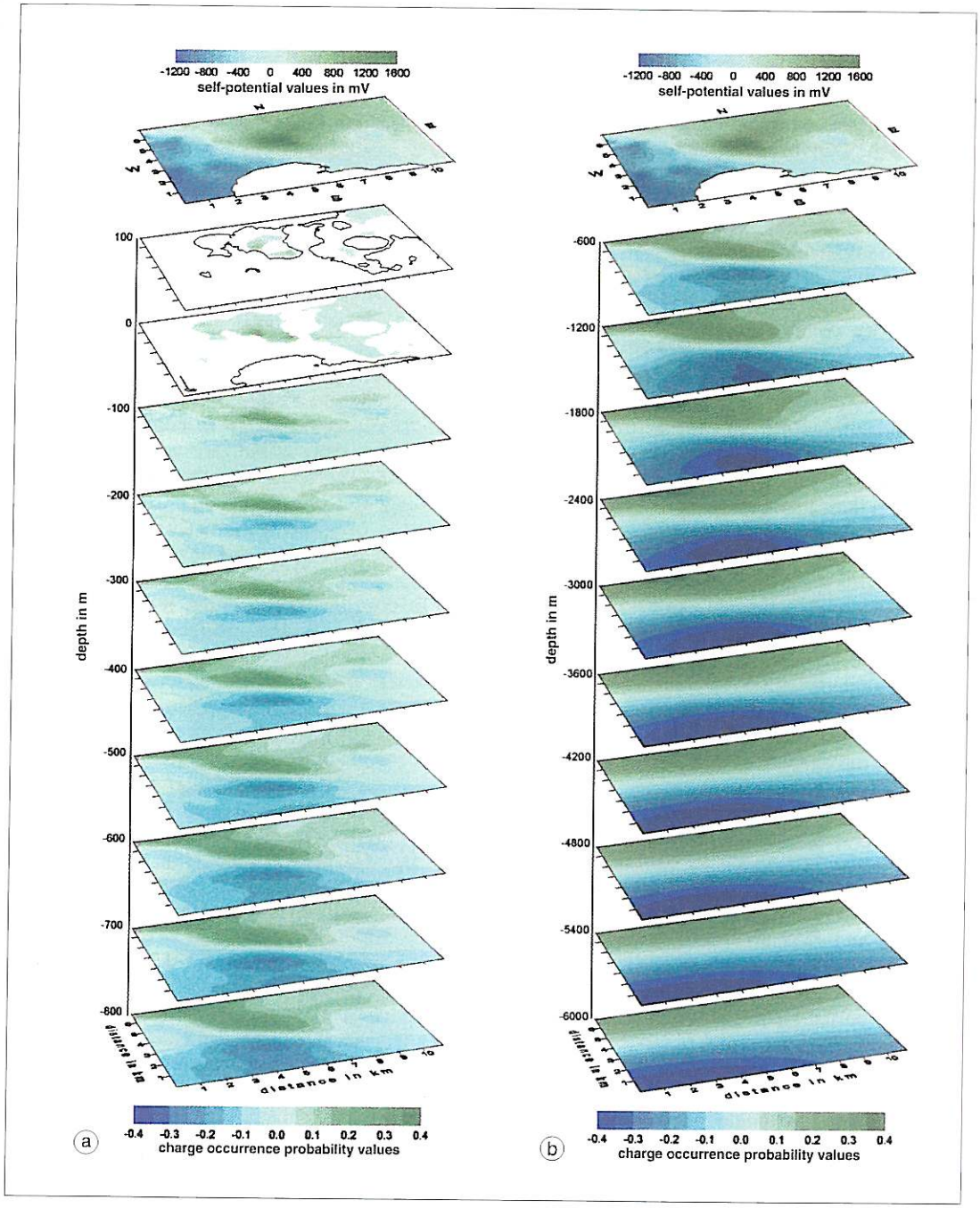

Fig. 9a,b. 3D self-potential probability tomography in the depth interval from: a) 100 m asl to 800 m bsl; b) 600 m bsl to 6000 m bsl.

race. According to the uniform patch model proposed by Fitterman (1979), the La Starza SP nuclei could be due to a streaming potential patch source likely located in the depth range 600-800 m bsl, where the maximum absolute values of the COP function related to the bipolar anomaly were obtained. The La Starza terrace would thus be the surface evidence of a thick vertical plate extending down to about 800 m bsl. The comparable intensity, shape and extent of the positive and negative clusters of the anomaly suggest that no hydraulic and electrical conductivity contrast should exist across the ENE-WSW trending thick vertical plate. This interpretation thus conforms with the hypothesis previously made about the existence of a N-S elongation direction of the 2D shallow resistive structure displayed by the MT-DG data within the CFc. Furthermore, the polarity of the two nuclei indicates that the streaming potential or electrokinetic coefficient sharply increases crossing the plate northwards.

As regards the deep features, fig. 9b shows a clear N-S oriented dipolar trend. The charge clusters have the highest absolute COP values in the range 1200-3600 m bsl for the northern positive nucleus and from 2400 m down to at least 6000 m bsl for the southern negative nucleus. A distance of about 6 km separates the centres of the two nuclei. The two charged clusters represent the SP regional pattern very well (fig. 8), although they are located at the margins of the survey area and most of the negative nucleus is located under the bay of Pozzuoli, where no field SP data were collected.

The pressure and temperature source model proposed by Fitterman (1979) can now be used for the interpretation of the deep CF SP anomaly. A simple configuration of this model consists of a buried spherical source body located near a vertical contact, which separates two quarter spaces generally characterised by different hydraulic and thermal conductivities and electrokinetic and thermoelectric coefficients (Di Maio and Patella, 1991). In the case of a sharp contrast of the electrokinetic and/or thermoelectric coefficient across the vertical contact from the source-holder quarter space to the outside quarter space, two features emerge: 1) the SP surface field is characterised by a negative anomaly above the spherical source and a positive anomaly on the other side of the vertical contact if there is an increase in the streaming potential and/or thermoelectric coefficient across the contact outwards; 2) the surface trace of the vertical contact corresponds to the zero-valued SP isoline.

Both the CF SP surface map (fig. 8) and the deep 3D COP tomography (fig. 9b) fit completely the features arising from Fitterman's distribution model. Therefore, a spheroid pressure and/or temperature source is likely to be located in the bay of Pozzuoli close to the coast at a hypocentral depth of not less than 5000 m bsl, where the largest probable accumulation of negative electrical charges occurs. Moreover, the vertical contact is likely to coincide with the imaged sequence of the zero-valued COP band from the surface (fig. 9a) downward (fig. 9b). This null COP band develops in a WNW-ESE direction over the whole survey area and includes in the middle the previously discussed La Starza volcano-tectonic feature.

To conclude this section, it is worth commenting on the results obtained from the analysis of ground deformation and seismic data collected during the bradyseismic crises of 1970-1984 and from temperature borehole data (T = 300-450 °C in the depth range 2-3 km bsl) (Bianchi *et al.*, 1986; Scandone *et al.*, 1991; Orsi *et al.*, 1999c; Wohletz *et al.*, 1999). In a review paper, Gasparini (1987) maintains that both ground movements and seismic activity can be explained assuming the existence of a magma body, around which a tensile and shear fracture zone with high permeability is supposed to develop due to pressure increase (fig. 10a). Variations of pore pressure inside this zone would significantly contribute to uplifting and sinking ground movements. Orsi *et al.* (1999c) maintain, instead, that this simple mechanical model cannot account for the occurrence of the intense seismic activity monitored during uplift and its absence during subsidence. They suggest a thermo-dynamical model (fig. 10b), in which a vertical fluid diffusion above a magma chamber is invoked to explain the variable behaviour between the central resurgent block and the peripheral part of the caldera floor. Subsidence is explained by a subsequent lateral fluid diffu-

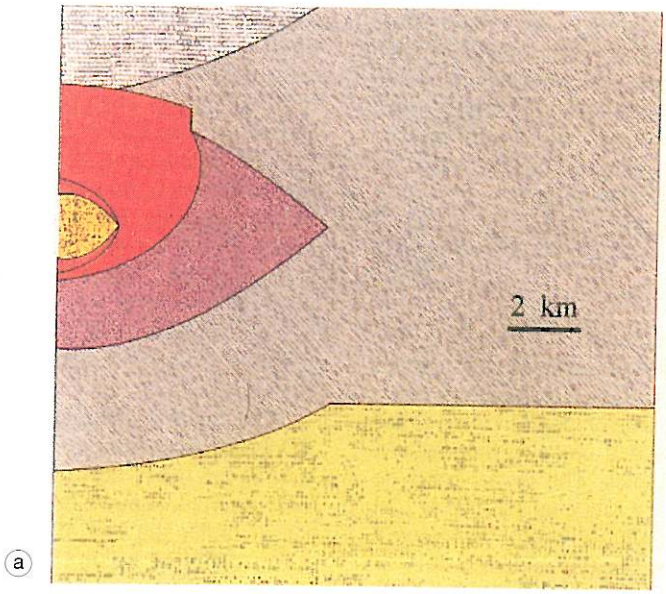

a

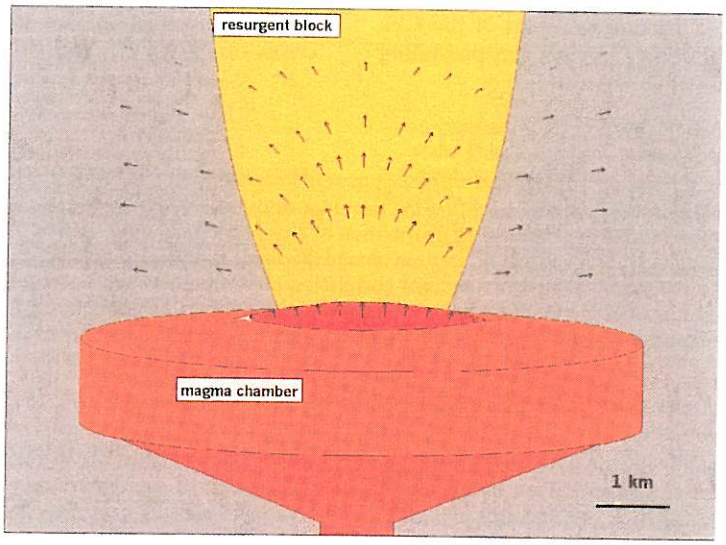

b

Fig. 10a,b. Schematic models of the Campi Flegrei magmatic system. a) The mechanical model (redrawn after Gasparini, 1987). Around the magma chamber (yellow zone) there are highly tensile (light red zone) and shear fractured bodies (red zone) that have low rigidity. These bodies are surrounded by material with rigidity from 3 to 15 times higher (violet zone). This more rigid material consists of volcanics at a temperature greater than 400 °C. Rigidity increases about 10 times more when temperature drops below 400 °C (grey zone). Finally, the white polka-dotted and green zones correspond with the low rigidity superficial pyroclastics and the brittle basement, respectively. The model has cylindrical symmetry around a vertical axis located in the bay of Pozzuoli. b) The thermo-dynamical model (redrawn after Orsi *et al.*, 1999c). Arrows indicate the flowage pattern of the shallow geothermal fluids in response to a temperature and/or pressure (volume) increase within the magma chamber.

sion, instead of a regression of the source pressures. As a matter of fact, both models invoke the presence of a magma chamber at a depth of 4 km under the bay of Pozzuoli, which conforms to the electrokinetic and thermoelectric source body that was previously introduced to explain the observed SP field map.

5. Conclusions

An analysis of MT and DG sounding data already available in literature, and of a recent SP ground survey of the CFc has allowed us to derive for the first time an electrical model of the caldera, which is located close to the western urban territory of Naples. The model must be considered preliminary, since no electric or EM data are currently available for the submerged portion of CFc under the Bay of Pozzuoli.

The analysis of all the available DG and MT soundings aligned along a N-S profile in the western sector of the emerged part of the CFc has given useful constraints on the prevailing dimensionality in the area. The result has been that the CFc is locally a prevailing 2D resistivity structure with a nearly N-S elongation direction. A similar analysis of the MT and DG soundings distributed along a nearly E-W profile has allowed us to draw a 2D electrical model that includes dispersive zones at the edges of the profile. These dispersive zones correspond to the known thermal areas of Mofete and Solfatara. The 2D E-W model has also revealed a resistive body with a prismatic cross-section in the middle of the profile, likely ascribable to dry volcanic filling sediments (La Starza block).

The most interesting result derived from a 3D probability tomography imaging of the SP data is the likely occurrence of a pressure and/or temperature source body of roughly spherical shape under the bay of Pozzuoli, centred at a mean depth of around 5 km bsl. This feature closely conforms to the magma body model previously inferred from ground deformation and seismic data related to the bradyseismic crises of 1970-1972 and 1982-1984.

Appendix

The SP probability tomography is based on the decomposition of a synthetic SP surface field into a sum of elementary contributions due to a discretised distribution of charge accumulation centres. The inversion problem consists in recovering the most probable discretised charge distribution underground, responsible of the measured SP field. The 3D tomography is based on a cross-correlation algorithm between a theoretical scanner function and the observed natural electric field. A charge occurrence probability (COP) function $\eta_S(x_q, y_q, z_q)$ is defined in the case of uneven topography as (Patella, 1997b)

$$\eta_S(x_q, y_q, z_q) = C_S \int_{-X}^{+X} \int_{-Y}^{+Y} \vec{E}_S[x, y, z(x,y)] \cdot \vec{\Im}_S[x - x_q, y - y_q, z(x,y) - z_q]\, g(z)\, dx\, dy, \tag{A.1}$$

where $\vec{E}_S$ is the natural electric field vector on the ground surface, $\vec{\Im}_S$ the scanner vector function, (x_q, y_q, z_q) is the tern of coordinates of a generic point in the subsoil, (x, y) is the pair of coordinates on a reference horizontal plane at sea level, $z(x, y)$ is the function representing the variable elevation on the survey surface S, whose projection onto the (x, y) reference plane is a rectangle with sides $2X$ and $2Y$, and $g(z)$ is the surface regularisation factor defined as

$$g(z) = [1 + (\partial z / \partial x)^2 + (\partial z / \partial y)^2]^{1/2}. \tag{A.2}$$

Furthermore, the modulus of $\vec{E}_S$ is explicated as follows:

$$E_S = \left[\left(\frac{\partial U}{\partial x} + \frac{\partial U}{\partial z} f_x(z) \right)^2 \frac{1}{1 + f_x^2(z)} + \left(\frac{\partial U}{\partial y} + \frac{\partial U}{\partial z} f_y(z) \right)^2 \frac{1}{1 + f_y^2(z)} \right]^{\frac{1}{2}} \tag{A.3}$$

and the modulus of $\vec{\Im}_S$ as

$$\Im_S = \left\{ \frac{[(x-x_q)+(z-z_q)f_x(z)]^2}{[(x-x_q)^2+(y-y_q)^2+(z-z_q)^2]^3} \frac{1}{1+f_x^2(z)} + \right.$$

$$\left. + \frac{[(y-y_q)+(z-z_q)f_y(z)]^2}{[(x-x_q)^2+(y-y_q)^2+(z-z_q)^2]^3} \frac{1}{1+f_y^2(z)} \right\}^{\frac{1}{2}}, \tag{A.4}$$

where $f_p(z)$, with p equal to either x or y, is the slope effect defined as

$$f_p(z) = \partial z / \partial p, \tag{A.5}$$

and U is the potential function of the SP field.

Finally, C_S is a normalisation coefficient given as

$$C_S = \left\{ \int_{-X}^{+X} \int_{-Y}^{+Y} E_S^2 [x, y, z(x,y)] g(z) dx dy \cdot \int_{-X}^{+X} \int_{-Y}^{+Y} \Im_S^2 [x, y, z(x,y) - z_q] g(z) dx dy \right\}^{-1/2}. \tag{A.6}$$

The function $\eta_S(x_q, y_q, z_q)$ is constrained to vary inside the interval $[-1, +1]$ (Patella, 1997b). Positive values for $\eta(x_q, y_q, z_q)$ are the result of a major influence from positive charge accumulations, while negative values result from negative charge concentrations.

REFERENCES

ASTER, R.C., R.P. MAYER, G. DE NATALE, A. ZOLLO, M. MARTINI, E. DEL PEZZO, R. SCARPA and G. IANNACCONE (1992): Seismic investigation of the Campi Flegrei. A summary and synthesis of results, in *Volcanic Seismology*, edited by P. GASPARINI, R. SCARPA and K. AKI, 462-483.

BARBERI, F., E. CASSANO, P. LA TORRE and A. SBRANA (1991): Structural evolution of Campi Flegrei caldera in light of volcanological and geophysical data, *J. Volcanol. Geotherm. Res.*, **48**, 33-49.

BERRINO, G., G. CORRADO, G. LUONGO and B. TORO (1984): Ground deformation and gravity change accompanying the 1982 Pozzuoli uplift, *Bull. Volcanol.*, **47**, 187-200.

BIANCHI, R., A. CORADINI, C. FEDERICO, G. GIBERTI, P. LANCIANO, J.P. POZZI, G. SARTORIS and R. SCANDONE (1986): Modeling of surface deformations in volcanic areas. The 1970-72 and 1982-84 crises of Campi Flegrei, Italy, *J. Geophys. Res.*, **92**, 14139-14150.

CASSANO, E. and P. LA TORRE (1987): Phlegrean Fields. Geophysics, *Quad. Ric. Sci.*, CNR, **114**, 103-131.

CHELINI, W. and A. SBRANA (1987): Phlegrean Fields. Subsurface geology, *Quad. Ric. Sci.*, CNR, **114**, 94-103.

CINQUE, A., G. ROLANDI and V. ZAMPARELLI (1984): L'estensione dei depositi marini olocenici nei Campi Flegrei in relazione alla vulcano-tettonica, *Boll. Soc. Geol. Ital.*, **104**, 327-348.

CORRADO, G., S. DE LORENZO, F. MONGELLI, A. TRAMACERE and G. ZITO (1998): Surface heat flow density at the Phlegrean Fields caldera (Southern Italy), *Geothermics*, **27**, 469-484.

DE NATALE, G. and F. PINGUE (1992): Seismological and geodetic data at Campi Flegrei (Southern Italy). Constraints on volcanological models, in *Volcanic Seismology*, edited by P. GASPARINI, R. SCARPA and K. AKI, 484-502.

DI GIROLAMO, P., M.R. CHIARA, L. LIRER, R. MUNNO, G. ROLANDI and D. STANZIONE (1984): Vulcanologia e petrologia dei Campi Flegrei, *Boll. Soc. Geol. Ital.*, **103**, 349-413.

DI MAIO, R. and D. PATELLA (1991): Basic theory of electrokinetic effects associated with earthquakes, *Boll. Geofis. Teor. Appl.*, **33**, 145-154.

DI MAIO, R., D. PATELLA and A. SINISCALCHI (1991): Sul problema del riconoscimento di uno strato elettricamente polarizzabile mediante misure magnetotelluriche, in *Proceedings of the 2nd Meeting of Geomagnetism and Aeronomy*, edited by A. MELONI and B. ZOLESI, ING, Roma, 239-250.

DI MAIO, R., V. DI SEVO, S. GIAMMETTI, D. PATELLA, S. PISCITELLI and C. SILENZIARIO (1996): Self-potential anomalies in some Italian volcanic areas, *Ann. Geofis.*, **39**, 179-188.

DI VITO, M.A., R. ISAIA, G. ORSI, J. SOUTHON, M. D'ANTONIO, S. DE VITA, L. PAPPALARDO and M. PIOCHI (1999): Volcanism and deformation since 12000 years at the Campi Flegrei caldera (Italy), *J. Volcanol. Geotherm. Res.*, **91**, 221-246.

FEDI, M., M.G. FIUME, V.A. LAPENNA, F. MONACO, D. PATELLA, A. RAPOLLA, N. ROBERTI, C. SATRIANO and A. SINISCALCHI (1986): Indagini geofisico-strutturali ed applicate per la modellizzazione della struttura flegrea, in *Atti del II Convegno «Bradisismo e Fenomeni Connessi»*, *Napoli*, 81-92.

FITTERMAN, D.V. (1979): Calculations of self-potential anomalies near vertical contacts, *Geophysics*, **44**, 195-205.

GASPARINI, P. (1987): Magmi in azione: Campi Flegrei, Long Valley, Rabaul, *Le Scienze*, **39**, 43-48.

GILLOT, P.Y., S. CHIESA, G. PASQUARÈ and L. VEZZOLI (1982): 33000 Yr. K/Ar dating of the volcano-tectonic horst of the isle of Ischia, gulf of Naples, *Nature*, **229**, 242-245.

HUNSCHE, U., A. RAPOLLA, G. MUSSMAN and L. ALFANO (1981): Application of magnetotelluric and DC electrical resistivity methods in the Neapolitan geothermal area, *J. Geophys.*, **49**, 26-34.

MARTINI, M., L. GIANNINI, A. BUCCIANTI, F. PRATI, P. CELLINI LEGITTIMO, P. IOZZELLI and B. CAPACCIONI (1991): Ten years of geochemical investigation at Phlegraean Fields (Italy), *J. Volcanol. Geotherm. Res.*, **48**, 161-171.

MAURIELLO, P., D. PATELLA and A. SINISCALCHI (1996): The magnetotelluric response over 2D media with resistivity frequency dispersion, *Geophys. Prospect.*, **44**, 789-818.

MONACO, F., D. PATELLA, A. RAPOLLA, N. ROBERTI and A. SINISCALCHI (1986): Prospezioni magnetotelluriche nei Campi Flegrei, *Bollettino del Gruppo Nazionale per la Vulcanologia*, CNR, Roma, 347-356.

ORSI, G., S. DE VITA and M. DI VITA (1996): The restless, resurgent Campi Flegrei nested caldera (Italy): constraints on its evolution and configuration, *J. Volcanol. Geotherm. Res.*, **74**, 179-214.

ORSI, G., L. CIVETTA, C. DEL GAUDIO, S. DE VITA, M. DI VITO, R. ISAIA, S.M. PETRAZZUOLI, G. RICCIARDI and C. RICCO (1999a): Short-term ground deformation and seismicity in the resurgent Campi Flegrei caldera (Italy): an example of active block-resurgence in a densely populated area, *J. Volcanol. Geotherm. Res.*, **91**, 415-451.

ORSI, G., D. PATELLA, M. PIOCHI and A. TRAMACERE (1999b): Magnetic modelling of the Phlegraean Volcanic District with extension to the Ponza archipelago, Italy, *J. Volcanol. Geotherm. Res.*, **91**, 345-360.

ORSI, G., S. PETRAZZUOLI and K. WOHLETZ (1999c): Thermo-fluid behaviour during unrest at the Campi Flegrei caldera (Italy), *J. Volcanol. Geotherm. Res.*, **91**, 453-470.

PARASNIS, D.S. (1997): *Principles of Applied Geophysics* (Chapman and Hall, London), pp. 429.

PATELLA, D. (1987): Tutorial. Interpretation of magnetotelluric measurements over an electrically dispersive one-dimensional earth, *Geophys. Prospect.*, **35**, 1-11.

PATELLA, D. (1993): I principi metodologici della magnetotellurica su mezzi generalmente dispersivi, *Ann. Geofis.*, **36** (suppl. n. 5/6), 147-160.

PATELLA, D. (1997a): Introduction to ground surface self-potential tomography, *Geophys. Prospect.*, **45**, 653-681.

PATELLA, D. (1997b): Self-potential global tomography including topographic effects, *Geophys. Prospect.*, **45**, 843-863.

PATELLA, D., A. TRAMACERE, R. DI MAIO and A. SINISCALCHI (1991): Experimental evidence of resistivity frequency-dispersion in magnetotellurics in the Newberry (Oregon), Snake River Plain (Idaho) and Campi Flegrei (Italy) volcano-geothermal Areas, *J. Volcanol. Geotherm. Res.*, **48**, 61-75.

POSTPISCHL, D. (1985): Catalogo dei terremoti italiani dall'anno 1000 al 1980, CNR-PFG, *Quad. Ric. Sci.*, **114-2B**, 1-238.

ROSI, M. and A. SBRANA (1987): Phlegrean Fields. Introduction, geological setting of the area, stratigraphy, description of mapped products, petrography, tectonics, *Quad. Ric. Sci.*, CNR, **114**, 9-93.

SCANDONE, R., F. BELLUCCI, L. LIRER and G. ROLANDI (1991): The structure of the Campanian plain and the activity of the Neapolitan volcanoes, *J. Volcanol. Geotherm. Res.*, **48**, 1-31.

WANNAMAKER, P.E., G.W. HOHMANN and S.H. WARD (1984): Magnetotelluric responses of three-dimensional bodies in layered Earth, *Geophysics*, **49**, 1517-1533.

WOHLETZ, K., L. CIVETTA and G. ORSI (1999): Thermal evolution of the Phlegraean magmatic system, *J. Volcanol. Geotherm. Res.*, **91**, 381-414.